

Supporting Information

Citral to Menthol Transformations in a Continuous Reactor over Ni/Mesoporous Aluminosilicate Extrudates Containing Sepiolite Clay Binder

Irina L. Simakova¹, Zuzana Vajglová², Päivi Mäki-Arvela², Kari Eränen², Leena Hupa²,
Markus Peurla³, Ermei M. Mäkilä³, Johan Wärnå², Dmitry Yu. Murzin^{2*}

¹ *Borshchov Institute of Catalysis, pr. Ak. Lavrentieva 5, 630090, Novosibirsk, Russia*

² *Åbo Akademi University, Johan Gadolin Process Chemistry Centre, Henrikinkatu 2, Turku/Åbo, Finland,
20500*

³ *University of Turku, FI-20520 Turku, Finland*

* *Corresponding author. E-mail: dmurzin@abo.fi*

Table of Contents

1. Characterization by N₂ physisorption (2)
 - Fig S1. Isotherms of powder Ni/MAS and extruded Ni/(MAS + sepiolite) catalysts (2)
 - Fig S2. Pore size distribution of powder Ni/MAS catalysts and Ni/(MAS + sepiolite) extrudates (2)
2. XRD data of powder Ni/MAS catalysts (3)
 - Table S1 The description of Ni/MAS powder catalysts (3)
 - Fig. S3. XRD patterns of powder Ni/MAS catalysts (4)
3. Kinetic modeling in continuous regime (5)
 - Fig. S4. Parity plots for all reaction components (5)
4. References (7)

1. Characterization by N₂ physisorption

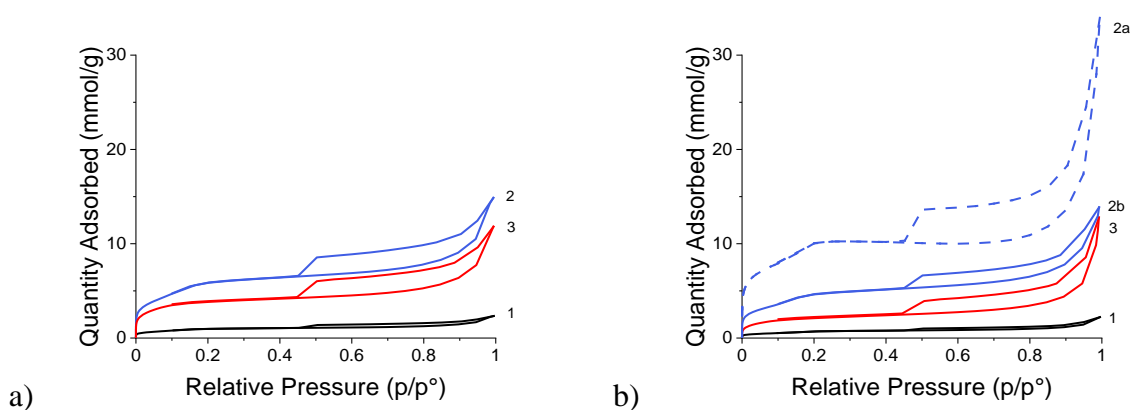


Figure S1. Isotherms of a) powder catalysts: 1 - Ni/MAS fresh non-reduced powder catalyst (black), 2 - Ni/MAS fresh reduced powder catalyst (blue), 3 - Ni/MAS spent powder catalyst (red); b) extrudates: 1 - Ni/(MAS+sepiolite) fresh non-reduced extrudates (black), 2a - Ni/(MAS+sepiolite) fresh reduced crushed extrudates (blue, dash line), 2b - Ni/(MAS+sepiolite) fresh reduced extrudates (blue, solid line), 3 - Ni/(MAS+sepiolite) spent extrudates (red).

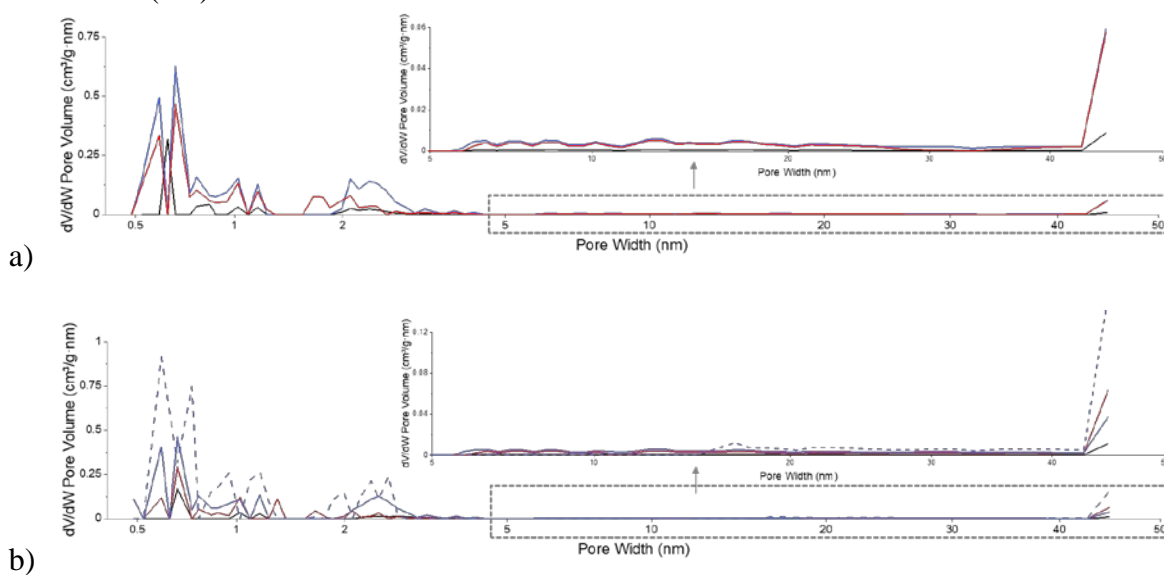


Figure S2. Pore size distribution of catalysts a) powder catalysts: 1 - Ni/MAS fresh non-reduced powder catalyst (black), 2 - Ni/MAS fresh reduced powder catalyst (blue), 3 - Ni/MAS spent powder catalyst (red); b) extrudates: 1 - Ni/(MAS+sepiolite) fresh non-reduced extrudates (black), 2a - Ni/(MAS+sepiolite) fresh reduced crushed extrudates (blue, dash line), 2b - Ni/(MAS+sepiolite) fresh reduced extrudates (blue, solid line), 3 - Ni/(MAS+sepiolite) spent extrudates (red).

2. XRD data of powder Ni/MAS catalysts

Powder XRD characterization of powdered catalysts was performed using PANalytical Empyrean diffractometer with five axis goniometer. The incident beam optics consisted of Bragg-Brentano HD x-ray mirror, fixed 1/4° divergence slit, 10 mm mask, 0.04 rad soller slit and 1° antiscatter slit. The diffracted beam optics consisted of 7.5 mm divergence slit, 0.04 rad soller slit and PIXcel detector array. The used X-ray tube was Empyrean Cu LFF. The X-ray radiation was filtered to include only Cu K α 1 and Cu K α 2 components. The results were analyzed with MAUD (Material Analysis Using Diffraction) analysis program [1]. Instrumental broadening was evaluated with Si standard sample. The measured samples are as listed in Table S1. The results were obtained with $\theta - 2\theta$ scan range from 5° to 120°.

Table S1. The description of Ni/MAS powder catalysts

#	Sample ID	Description
1	5%-Ni/H-MCM-41 PF	Powder fresh non-reduced
2	5%-Ni/H-MCM-41 PFR	Powder fresh reduced
3	5%-Ni/H-MCM-41 PS	Powder spent

The results for 5%-Ni H-MCM-41 PF, 5%-Ni H-MCM-41 PFR and 5%-Ni H-MCM-41 PS are presented in Figure S3. Figure S3 includes also the standardized diffraction patterns for Ni [2] and NiO [3]. The diffraction patterns presented in Figure S3 show a clear contribution from Ni in 5%-Ni H-MCM-41 PFR and 5%-Ni H-MCM-41 PS and NiO in 5%-Ni H-MCM-41 PF and 5%-Ni H-MCM-41 PFR. The peaks close 44.5°, 51.8°, 76.4° and 93.0° are assigned to Ni phase and the peaks close to 37.2°, 43.3°, 62.8°, 75.4° and 79.4° to NiO. All the samples show also a broad diffraction peak close 20°.

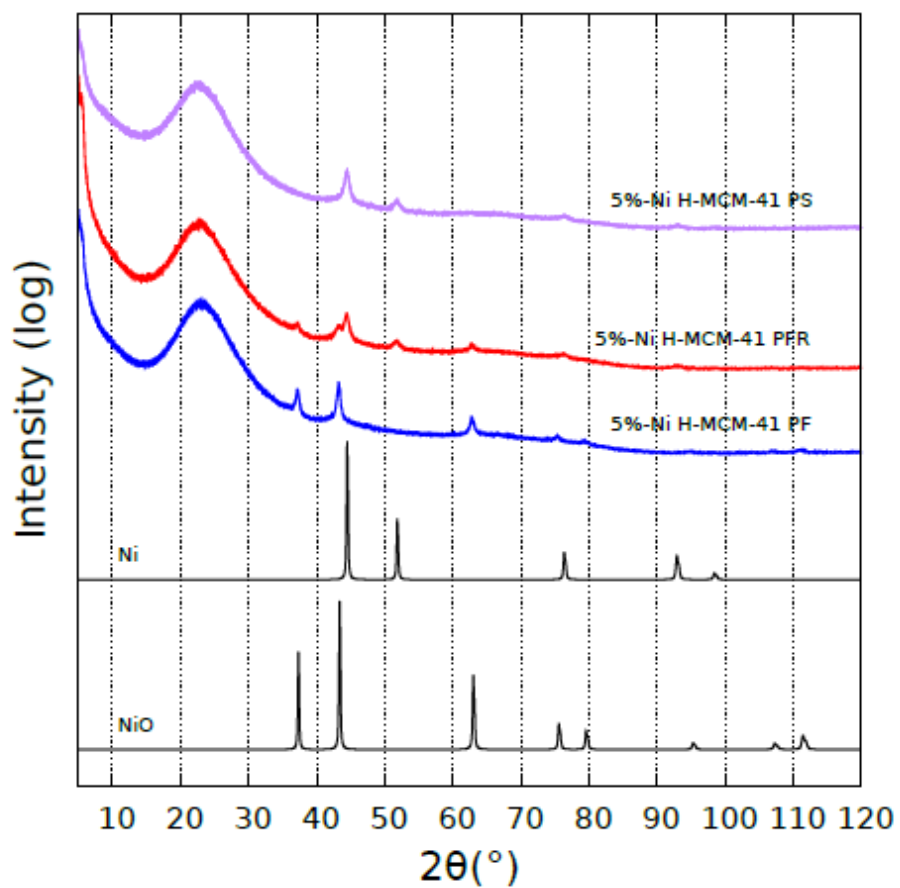
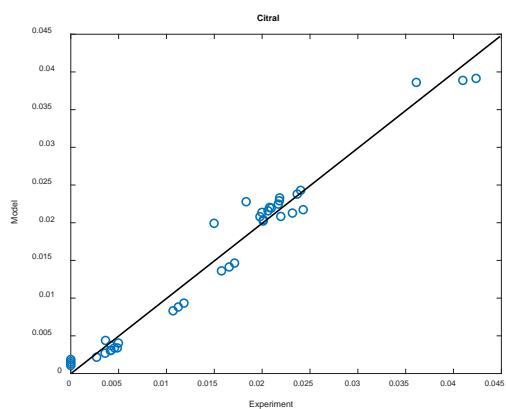
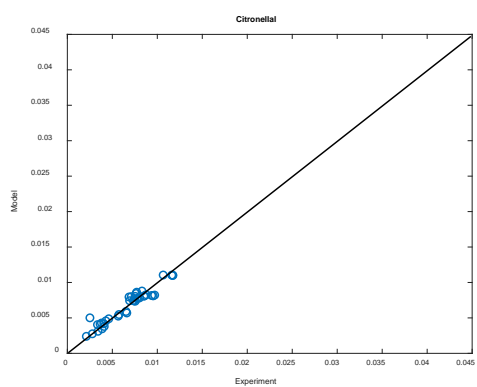


Figure S3. Combined results for 5%-Ni H-MCM-41 PF, 5%-Ni H-MCM-41 PFR and 5%-Ni H-MCM-41 PS along with standardized diffraction data for Ni and NiO.

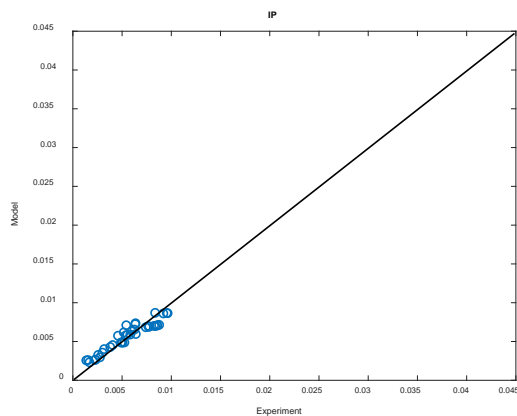
3. Kinetic modeling in continuous regime



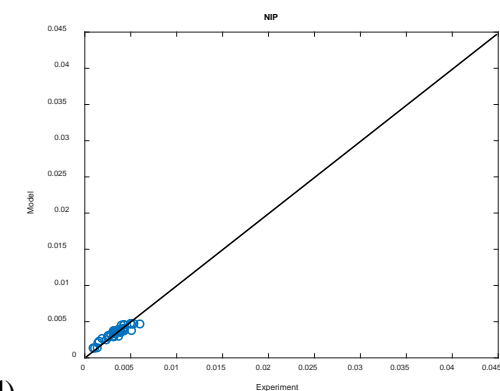
a)



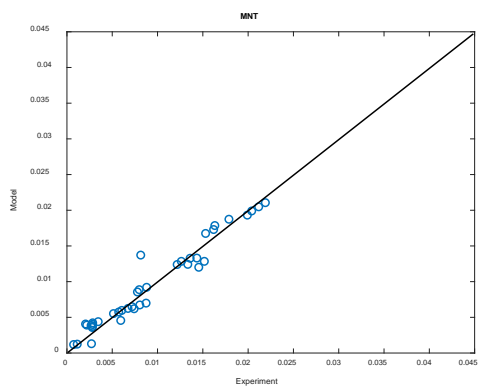
b)



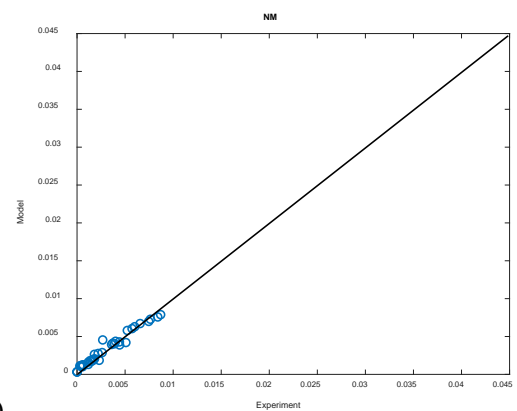
c)



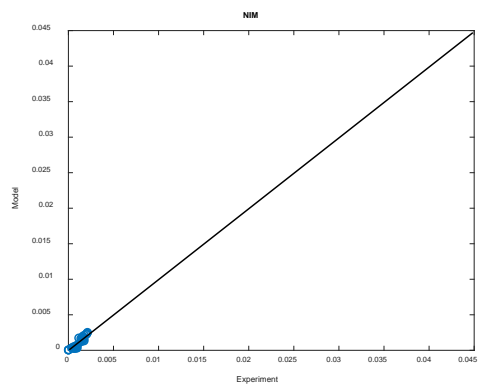
d)



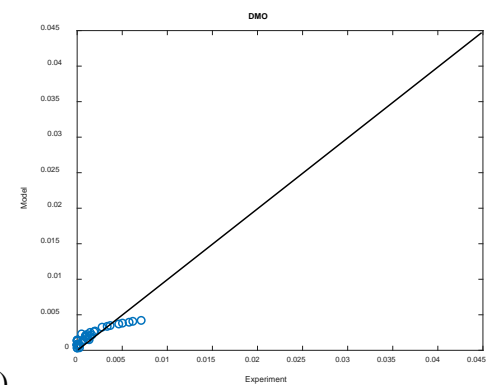
e)



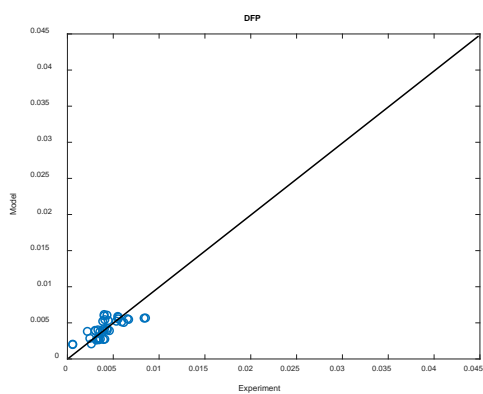
f)



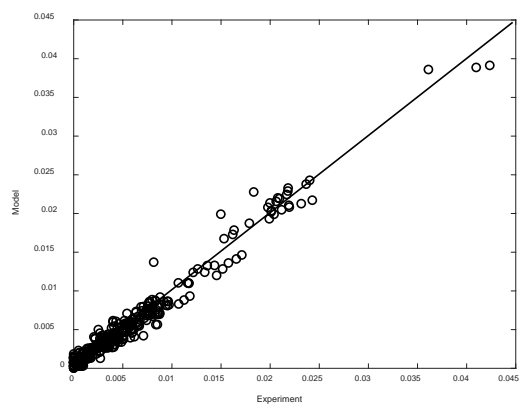
g)



h)



i)



j)

Figure S4. Parity plots for a) citral, b) citronella, c) isopulegol, d) neoisopulegol, e) menthol, f) neomenthol, g) neoisomenthol, h) dimethyloctanol, i) defunctionalized products, j) all products together.

4. References

- [1] L. Lutterotti, Total pattern fitting for the combined size-strain-stress-texture determination in thin film diffraction, Nuclear Inst. and Methods in Physics Research, B, 268, 334-340, 2010.
- [2] Wyckoff, R. W. G. Second edition. Interscience Publishers, New York, New York Crystal Structures (1963) 1, (p. 7-83).
- [3] Wyckoff, R. W. G. Second edition. Interscience Publishers, New York, New York Crystal Structures (1963) 1, (p. 85-237).